ISSN 0915-633X

NATIONAL INSTITUTE FOR FUSION SCIENCE

Molecular Dynamics Simulation of Structural Formation of Short Polymer Chains

S. Fujiwara and T. Sato

(Received - July 25, 1997)

NIFS-504 Aug. 1997

RESEARCH REPORT
NIFS Series

NAGOYA, JAPAN

Molecular Dynamics Simulation of Structural Formation of Short Polymer Chains

Susumu Fujiwara and Tetsuya Sato

Theory and Computer Simulation Center, National Institute for Fusion Science, 322-6, Oroshi-cho, Toki 509-52, Japan

Abstract

Molecular dynamics simulations are carried out to study the structural formation of 100 short polymer chains, each of which consists of 20 CH_2 groups. Our simulations show that the orientationally ordered structure at 400 K is formed from a random structure at 700 K by cooling. The essentially extended chains form a monolayer structure with a hexagonal packing. It is ascertained that the formation of the ordered structure proceeds stepwise in connection with the manner in which the local ordered regions grow. The stepwise behavior is also found in the time variation of the van der Waals energy.

Keywords: molecular dynamics simulation, polymer chain, structural formation, bond-orientational order

The crystal structure of the rotator phase of n-alkanes, which are typical of short polymer chains with simple chemical structure, has been extensively studied by experiments [1–16], theoretical analyses [17,18], and computer simulations [19–25] from physical, chemical, and biological interests. Several experimental techniques including x-ray diffraction [1–8], infrared and Raman spectroscopy [9–11], neutron scattering [12–14], and NMR [15,16] have been used to reveal interesting features of the molecular packing, intramolecular defects and molecular motions in the rotator phase of n-alkanes. The crystal structures of the rotator phase of odd-numbered n-alkanes from $C_{11}H_{24}$ to $C_{25}H_{52}$ have been carefully investigated by Doucet *et al.* [3–6] and Ungar [7]. With increasing temperature, shorter n-alkanes up to $C_{21}H_{44}$ transform from an ordered, orthorhombic structure to a disordered, face-centered-orthorhombic (FCO), rotator phase (referred to as $R_{\rm I}$ or FCO phase) with orthorhombic subcell. Longer n-alkanes ($C_{23}H_{48}$ and $C_{25}H_{52}$) show another rotator phase (referred to as $R_{\rm II}$ or hexagonal phase) with hexagonal subcell above the $R_{\rm I}$ phase. The $R_{\rm I}$ phase has a bilayer structure while the $R_{\rm II}$ phase has a trilayer structure. In the $R_{\rm I}$ phase, the ratio of the lattice constants a/b varies rapidly with temperature from the ordinary orthorhombic value of about 1.5 to the hexagonal value $\sqrt{3}$.

Structures and molecular motions in the rotator phases of n-alkanes have been studied by Monte Carlo simulations [19–21] and molecular dynamics simulations [22–24]. In the $R_{\rm I}$ phase, each chain has four possible orientations. By contrast, in the $R_{\rm II}$ phase, each chain has six equivalent orientations and the molecules make sporadic large rotations to the different directions. The longitudinal motion of the molecules is very active and independent of the rotational motion. The crystals in the rotator phases are composed of many ordered domains within which the chains tend to parallel their zigzag planes to one of the four or six directions. A significant number of conformational defects develop predominantly at the chain ends. Esselink *et al.* carried out MD simulations of nucleation and melting of bulk n-alkane systems in order to determine the crystallization and melting temperatures [25]. They introduced a new method to identify crystalline regions and computed the crystallization rate of a nucleus.

The purpose of this Letter is to clarify the dynamical processes of the structural formation of short polymer chains at the molecular level. With a view to investigating the transition process of short polymer chains from a random structure to the orientationally ordered structure, we perform the MD simulations of 100 short polymer chains and analyze the growth process of the local orientationally-ordered regions (clusters). We believe that our simulation results can provide an essential clue to understand the molecular motion in the metastable hexagonal phase whose importance in crystal growth has been recently pointed out [26].

The present computational model is the same as that used in the previous work on the structural formation of a single long polymer chain [27]. The model polymer chain consists of a sequence of CH_2 groups, which are treated as united atoms. In reality, the hydrogen atoms must be explicitly considered [24,28]. Since we are concerned with the dynamical formation process of the orientationally ordered structure in this study, we adopt the united atom approximation. The united atoms interact via the bonded potentials (bond-stretching, bond-bending and torsional potentials) and the van der Waals non-bonded potential (12-6 Lennard-Jones potential). The atomic force field used here is the DREIDING potential [29]. The numerical integrations of the equations of motion are performed using the velocity version of the Verlet algorithm [30]. We apply the Nosé-Hoover method in order to keep the temperature of the system constant [31–33]. The integration time step and the relaxation constant for the heat bath variable are 0.001 ps and 0.1 ps, respectively. The cutoff distance for the Lennard-Jones potential is 10.5 Å. The total momentum and the total angular momentum are taken to be zero in order to cancel overall translation and rotation of chains. At first, we prepare random configuration of 100 short polymer chains, each of which consists of 20 CH_2 groups, at high temperature ($T = 700$ K). It is then quenched to $T = 400$ K and the MD simulations are performed for 2000 ps.

We show, in Fig. 1, the chain configurations at various times ($t = 1$, 200, 300 and 2000 ps) obtained by our MD simulations at $T = 400$ K. The x, y, and z axes in this figure respectively correspond to the crystalline a, b, and c axes in the orthorhombic system. The

unit vector parallel to the z axis is defined as the eigenvector corresponding to the largest eigenvalue of an orientational order parameter tensor $\mathbf{Q}$ which is constructed by

$$Q_{\alpha\beta} = \left\langle \langle \hat{u}_{m\alpha} \hat{u}_{m\beta} \rangle_{\text{inner}} \right\rangle - \frac{1}{3}\delta_{\alpha\beta}, \tag{1}$$

where $\alpha, \beta = x, y, z$, $\hat{\mathbf{u}}_m$ is a unit vector directed along the principal axis with the smallest moment of inertia of the m-th chain, and $\langle \cdots \rangle$ and $\langle \cdots \rangle_{\text{inner}}$ denote the time average and the average over the inner 37 chains (Fig. 2), respectively. The time average is performed between 1500 and 2000 ps. The x and y axes are determined from the individual average central positions of the inner chains between 1500 and 2000 ps. The lattice constants a and b are calculated as $a = 0.750$ nm and $b = 0.432$ nm, respectively. Since the ratio a/b is equal to $1.735 \approx \sqrt{3}$, polymer chains are found to be packed hexagonally (Fig. 2). From Fig. 1, we find the following features: (i) In the early time ($t = 1$ ps), *gauche* states (deep green to light blue) are excited in various places and the configuration of the polymer chains is *random*. (ii) With the elapse of time, the local orientationally-ordered regions (clusters) grow in several positions ($t = 200$ ps) and at last they coalesce into a large cluster ($t = 300$ ps). (iii) At $t = 2000$ ps, a highly ordered structure is formed. Almost all the bonds are in the *trans* state and the *gauche* defects are located exclusively in the chain ends.

The Lennard-Jones energy E_{LJ} is plotted in Fig. 3 as a function of time. This figure indicates that there are two time regions (A and B) in which E_{LJ} drops rapidly after $t = 50$ ps. The structural formation is expected to proceed in these time regions. In order to investigate the growth process of the global bond-orientational order, we calculate the global bond-orientational order parameter S, which is defined by

$$S = \frac{1}{N(n-2)} \sum_{m=1}^{N} \sum_{i=3}^{n} \frac{3\cos^2 \psi_i^m - 1}{2}, \tag{2}$$

where N and n are respectively the number of polymer chains and the number of CH_2 groups per polymer chain ($N = 100$, $n = 20$) and ψ_i^m is the angle between the sub-bond vector of the m-th chain $\mathbf{b}_i^m$ and the z axis. The sub-bond vector $\mathbf{b}_i^m = (\mathbf{r}_i^m - \mathbf{r}_{i-2}^m)/2$ is the vector formed by connecting centers of two adjacent bonds i and $i-1$ of the m-th chain

and $\mathbf{r}_i^m$ represents the position vector of the i-th atom of the m-th chain. The parameter S would take a value of 1.0, 0.0 or -0.5, respectively, for polymer chains whose sub-bonds are perfectly parallel, random or perpendicular to the z axis. We show the time dependence of the global bond-orientational order parameter S in Fig. 4. Up to $t = 150$ ps, the parameter S takes a value near zero, which shows that there is no global bond-orientational order in this time region. After $t = 150$ ps, S increases sharply and reaches about 0.8 in the time region B. After that, S increases gradually and reaches its asymptotic value of about 0.9 at $t \approx 700$ ps. It is also found that the global bond-orientational order starts to grow in the time region A.

In order to investigate the *local* orientational order, we next introduce the concept of "*cluster*" according to Ref. [25]. The definition of "cluster" is as follows. Two polymer chains belong to the same cluster if the following two conditions are satisfied: (i) $|\mathbf{r}_c^i - \mathbf{r}_c^j| < r_0$ and (ii) $\alpha_{ij} < \alpha_0$, where $\mathbf{r}_c^i$ is the position vector of the center of mass of the i-th chain, α_{ij} is the angle between the principal axis with the smallest moment of inertia of the i-th chain and that of the j-th chain and satisfies $0 < \alpha_{ij} < \pi/2$. In our calculations, we set $r_0 = 1.5\sigma$ ($\sigma = 0.36239$ nm) and $\alpha_0 = 10°$. We show, in Fig. 5, the number of polymer chains in the largest and second largest cluster as a function of time. Only small clusters whose size is smaller than 10 can be seen up to $t = 120$ ps. In the time region A, the size of clusters increases rapidly and the size of the largest cluster becomes over 30. The orientation of clusters as a whole is random in this time region because the global bond-orientational order parameter is almost zero (Fig. 4). After that, the size of the largest cluster only fluctuates around a mean value until $t = 210$ ps. On the other hand, the global bond-orientational order grows rapidly in this time region (Fig. 4). Therefore, the orientations of individual clusters are considered to become parallel to one another in this time region. In the time region B, the size of the largest cluster increases rapidly while the size of the second largest cluster decreases. Several middle-sized clusters whose size is larger than 10 are found to coalesce into a large cluster. After the coalescence of clusters, the size of the largest cluster increases gradually until it reaches its maximum value of 100 at

$t \approx 700$ ps. It is worth mentioning that the stepwise behavior in the time variation of the Lennard-Jones energy and the size of the largest cluster was also observed in the simulation results by Esselink *et al.* [25].

In summary, by carrying out MD simulations of 100 short polymer chains and analyzing the growth process of clusters, we have obtained the following new results:

(1) The orientationally ordered structure at $T = 400$ K is formed from a random structure at $T = 700$ K by cooling. The essentially extended chains form an orientationally ordered structure with a hexagonal packing and the *gauche* defects are located exclusively in the chain ends.

(2) In the formation process of the ordered structure, the Lennard-Jones energy decreases stepwise. The stepwise behavior has a close connection with that of the growth of the local ordered clusters.

(3) The formation of the ordered structure proceeds as follows: (i) Only small clusters whose size is smaller than 10 are formed in various places ($t < 120$ ps). (ii) Several middle-sized clusters whose size is between 10 and 40 are formed ($120 < t < 210$ ps). (iii) Middle-sized clusters coalesce into a large cluster ($210 < t < 300$ ps). (iv) After that, the cluster gradually grows larger until the size of the cluster reaches its maximum value of 100 at $t \approx 700$ ps.

In this study, we dealt with the short polymer chains in order to ignore the effects of the entanglement. As a result, the obtained orientationally-ordered structure was a monolayer structure in which the essentially extended chains aggregated two-dimensionally. We will carry out MD simulations of long polymer chains in order to investigate the effect of the entanglement on the structural formation.

This work was partially supported by a Grant-in-Aid for Scientific Research on Priority Areas, Cooperative Phenomena in Complex Liquids, from the Ministry of Education, Science, Sports and Culture. This work was carried out by using the Advanced Computing System for Complexity Simulation (NEC SX-3/24R) at the NIFS.

REFERENCES

[1] A. Müller, Proc. R. Soc. A **138**, 514 (1932).

[2] B. Ewen, G. Strobl, and D. Richter, J. Chem. Soc. Faraday Discuss. **69**, 19 (1980).

[3] J. Doucet, I. Denicolo, and A.F. Craievich, J. Chem. Phys. **75**, 1523 (1981); J. Doucet, I. Denicolo, A.F. Craievich, and A. Collet, *ibid.* **75**, 5125 (1981).

[4] I. Denicolo, J. Doucet, and A.F. Craievich, J. Chem. Phys. **78**, 1465 (1983).

[5] J. Doucet, I. Denicolo, A.F. Craievich, and C. Germain, J. Chem. Phys. **80**, 1647 (1984).

[6] A.F. Craievich, I. Denicolo, and J. Doucet, Phys. Rev. B **30**, 4782 (1984).

[7] G. Ungar, J. Phys. Chem. **87**, 689 (1983).

[8] T. Yamamoto, K. Nozaki, and T. Hara, J. Chem. Phys. **92**, 631 (1990).

[9] G. Zerbi, R. Magni, M. Gussoni, K.H. Moritz, A. Bigotto, and S. Dirlikov, J. Chem. Phys. **75**, 3175 (1981).

[10] M. Maroncelli, H.L. Strauss, and R.G. Snyder, J. Chem. Phys. **82**, 2811 (1985).

[11] M. Maroncelli, S.P. Qi, H.L. Strauss, and R.G. Snyder, J. Am. Chem. Soc. **104**, 6237 (1982).

[12] B. Ewen and D. Richter, J. Chem. Phys. **69**, 2954 (1978).

[13] J. Doucet and A.J. Dianoux, J. Chem. Phys. **81**, 5043 (1984).

[14] F. Guillaume, J. Doucet, C. Sourisseau, and A.J. Dianoux, J. Chem. Phys. **91**, 2555 (1989).

[15] M. Stohrer and F. Noack, J. Chem. Phys. **67**, 3729 (1977).

[16] M.G. Taylor, E.C. Kelusky, I.C.P. Smith, H.L. Casal, and D.G. Cameron, J. Chem. Phys. **78**, 5108 (1983).

[17] A. Holz, J. Naghizadeh, and D.T. Vigren, Phys. Rev. B **27**, 512 (1983).

[18] T. Bleha and J. Gajdos, Colloid Polym. Sci. **265**, 574 (1987).

[19] T. Yamamoto, J. Chem. Phys. **82**, 3790 (1985); **89**, 2356 (1988).

[20] T. Yamamoto, M. Hikosaka, and N. Takahashi, Macromolecules **27**, 1466 (1994).

[21] T. Yamamoto, J. Chem. Soc. Faraday Trans. **91**, 2559 (1995).

[22] J.P. Ryckaert and M.L. Klein, J. Chem. Phys. **85**, 1613 (1986).

[23] J.P. Ryckaert, M.L. Klein, and I.R. McDonald, Phys. Rev. Lett. **58**, 698 (1987).

[24] J.P. Ryckaert, I.R. McDonald, and M.L. Klein, Molecular Physics **67**, 957 (1989).

[25] K. Esselink, P.A.J. Hilbers, and B.W.H. van Beest, J. Chem. Phys. **101**, 9033 (1990).

[26] M. Hikosaka, S. Rastogi, A. Keller, and H. Kawabata, J. Macromol. Sci. Phys. **B31**, 87 (1992).

[27] S. Fujiwara and T. Sato, J. Chem. Phys. **107**, 613 (1997).

[28] D.E. Williams, J. Chem. Phys. **47**, 4680 (1967).

[29] S.L. Mayo, B.D. Olafson, and W.A. Goddard III, J. Phys. Chem. **94**, 8897 (1990).

[30] L. Verlet, Phys. Rev. **159**, 98 (1967).

[31] S. Nosé, Mol. Phys. **52**, 255 (1984).

[32] S. Nosé, J. Chem. Phys. **81**, 511 (1984).

[33] W.G. Hoover, Phys. Rev. A **31**, 1695 (1985).

FIGURES

FIG. 1. The chain configurations of 100 short polymer chains at various times: $t = 1, 200, 300,$ and 2000 ps (from left to right). Top and bottom figures are respectively viewd along the z axis and the y axis. Color denotes the absolute value of the dihedral angle around each bond and the end bonds are colored with blue.

FIG. 2. The center-of-mass positions of individual polymer chains viewd along the z axis averaged between 1500 and 2000 ps. The lattice constants a and b are respectively $a = 0.750$ nm and $b = 0.432$ nm. Hexagons are depicted in order to show a hexagonal packing of the polymer chains. "Inner chains" are defined as the central 37 chains within a thick hexagon.

FIG. 3. The Lennard-Jones energy E_{LJ} vs. time t. Letters A and B denote the time regions where E_{LJ} decreases rapidly.

FIG. 4. The global bond-orientational order parameter S vs. time t. Letters A and B are explained in the caption of Fig. 3.

FIG. 5. The size of the largest and second largest cluster vs. time t. Letters A and B are explained in the caption of Fig. 3.

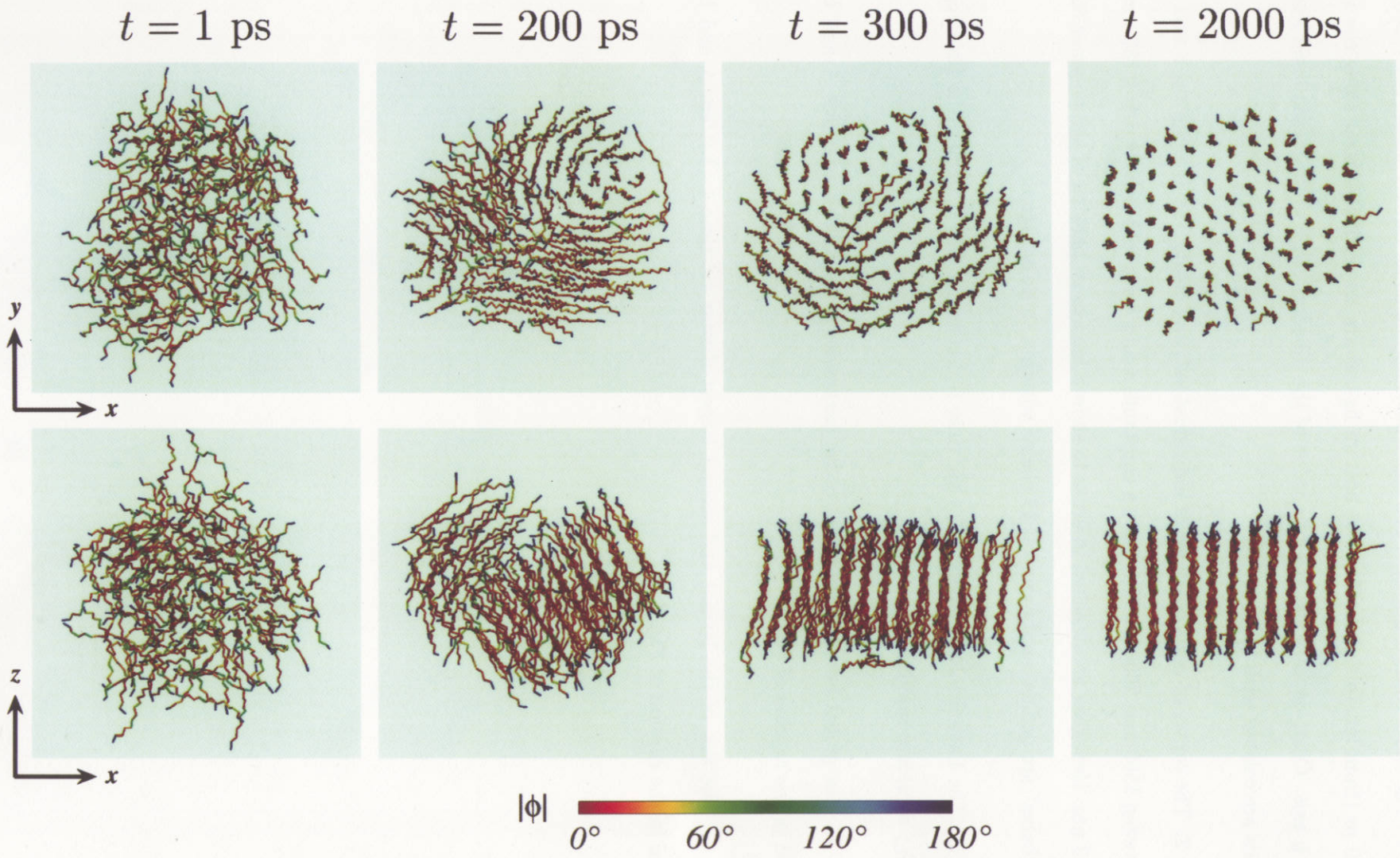

Fig. 1

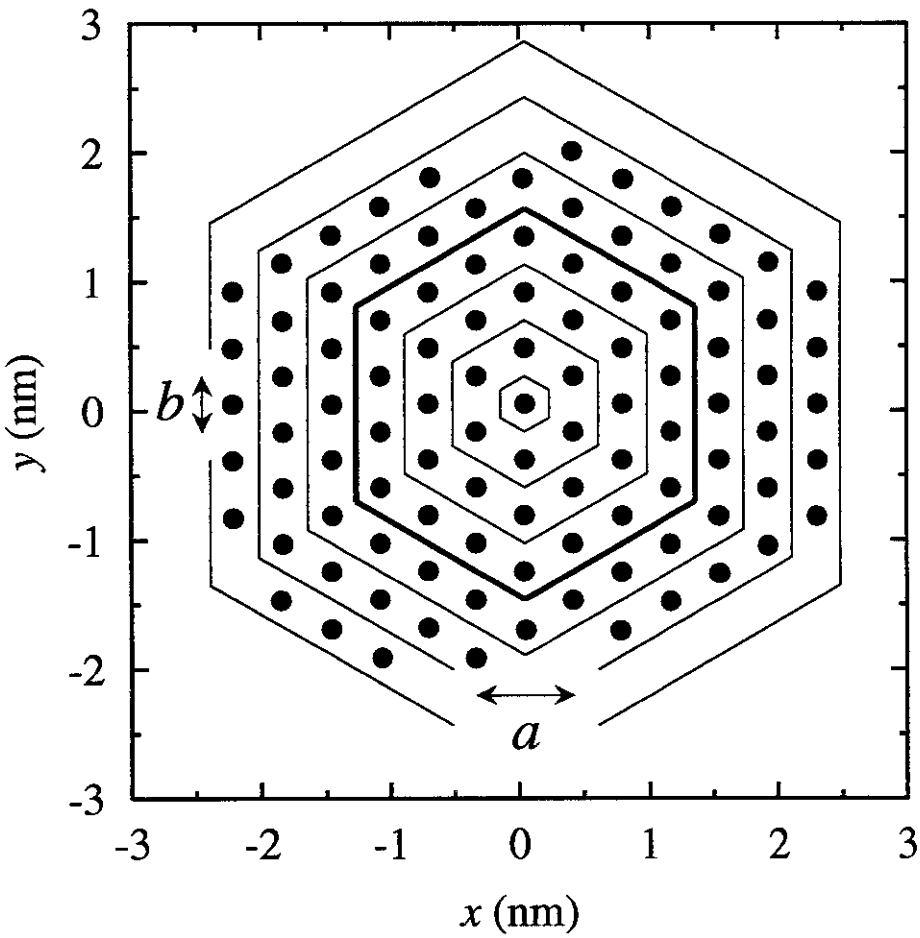

Fig. 2

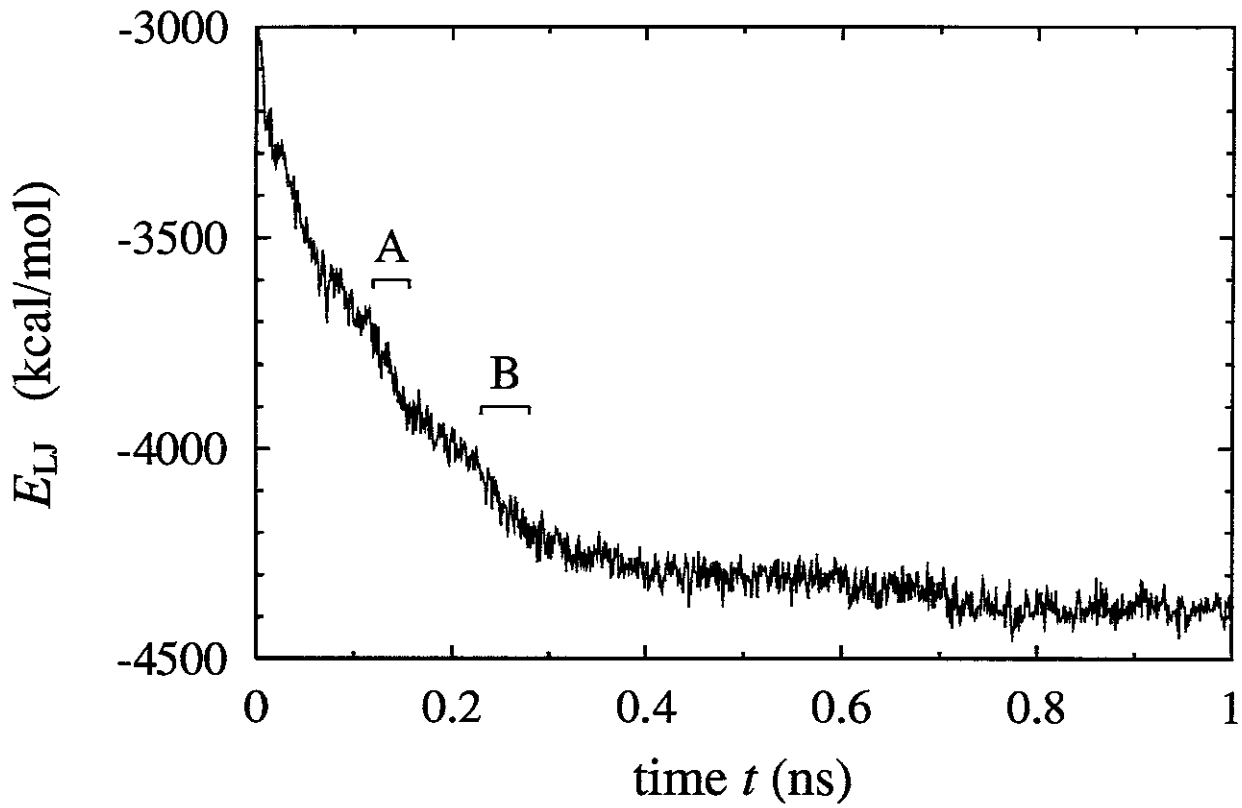

Fig. 3

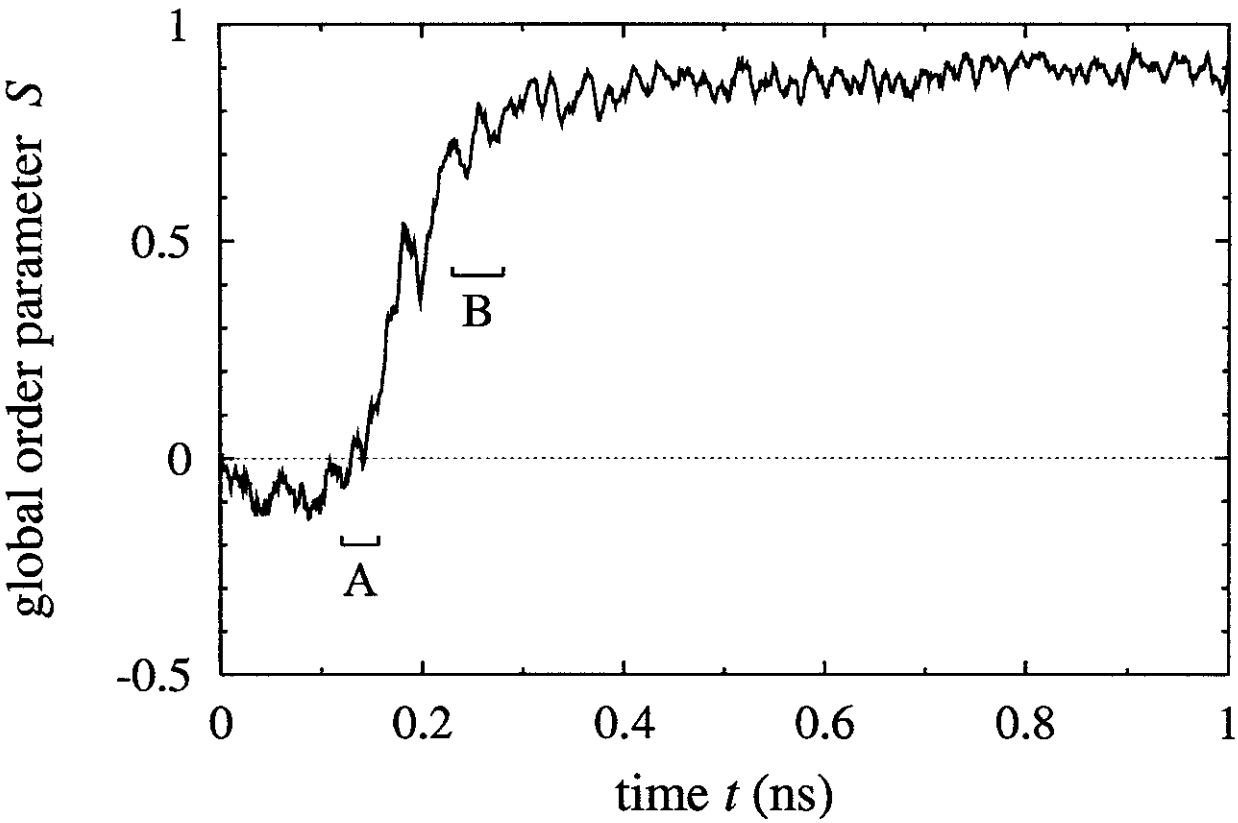

Fig. 4

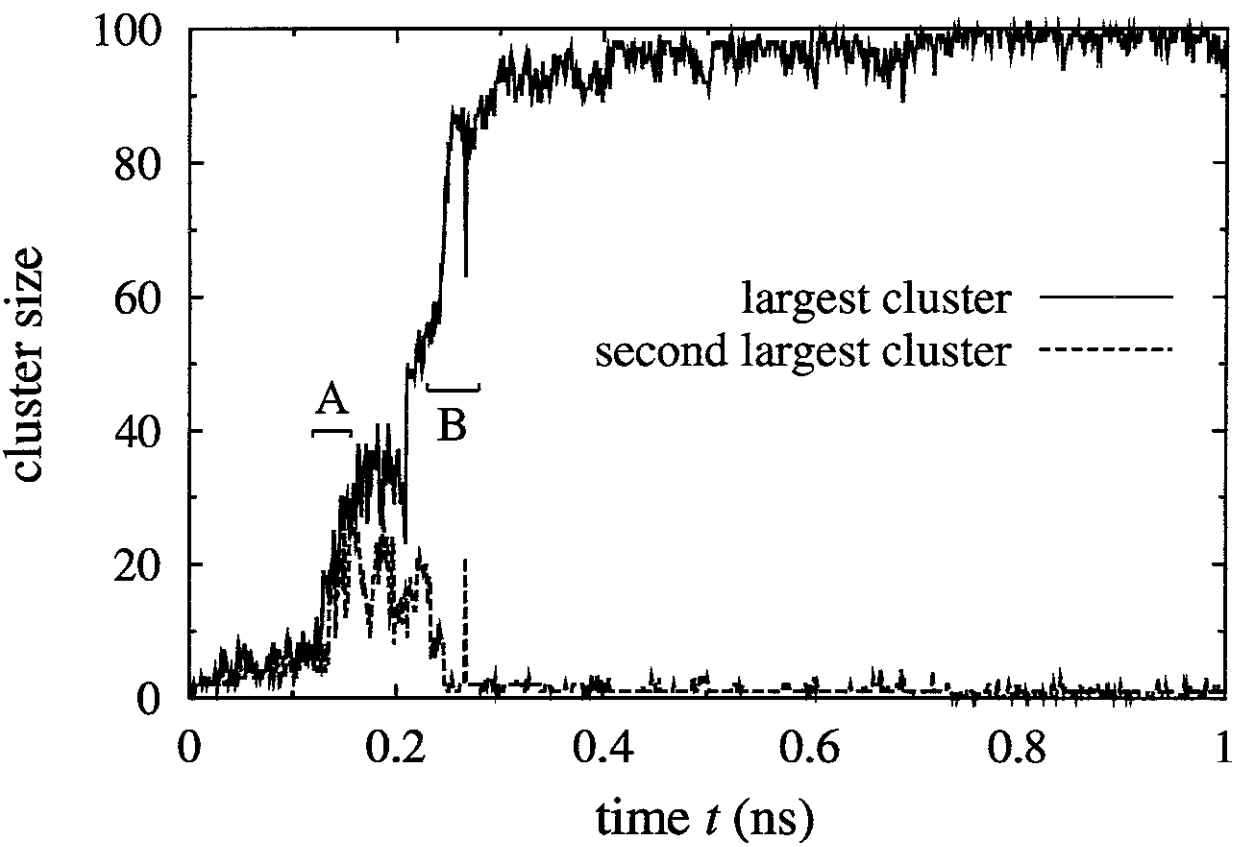
100
80
60
40
20
0
cluster size
largest cluster
second largest cluster
A
B
0
0.2
0.4
0.6
0.8
1
time t (ns)

Fig. 5

Recent Issues of NIFS Series

NIFS-458 A Kageyama and T. Sato,
Generation Mechanism of a Dipole Field by a Magnetohydrodynamic Dynamo; Oct. 1996

NIFS-459 K. Araki, J. Mizushima and S. Yanase,
The Non-axisymmetric Instability of the Wide-Gap Spherical Couette Flow; Oct. 1996

NIFS-460 Y. Hamada, A. Fujisawa, H. Iguchi, A. Nishizawa and Y. Kawasumi,
A Tandem Parallel Plate Analyzer; Nov. 1996

NIFS-461 Y. Hamada, A. Nishizawa, Y. Kawasumi, A. Fujisawa, K. Narihara, K. Ida, A. Ejiri, S. Ohdachi, K. Kawahata, K. Toi, K. Sato, T. Seki, H. Iguchi, K. Adachi, S. Hidekuma, S.Hirokura, K. Iwasaki, T. Ido, M. Kojima, J. Koong, R. Kumazawa, H. Kuramoto, T. Minami, I. Nomura, H. Sakakita, M. Sasao, K.N. Sato, T. Tsuzuki, J. Xu, I. Yamada and T. Watari,
Density Fluctuation in JIPP T-IIU Tokamak Plasmas Measured by a Heavy Ion Beam Probe; Nov. 1996

NIFS-462 N. Katsuragawa, H. Hojo and A. Mase,
Simulation Study on Cross Polarization Scattering of Ultrashort-Pulse Electromagnetic Waves; Nov. 1996

NIFS-463 V. Voitsenya, V. Konovalov, O. Motojima, K. Narihara, M. Becker and B. Schunke,
Evaluations of Different Metals for Manufacturing Mirrors of Thomson Scattering System for the LHD Divertor Plasma; Nov. 1996

NIFS-464 M. Pereyaslavets, M. Sato, T. Shimozuma, Y. Takita, H. Idei, S. Kubo, K. Ohkubo and K. Hayashi,
Development and Simulation of RF Components for High Power Millimeter Wave Gyrotrons; Nov. 1996

NIFS-465 V.S. Voitsenya, S. Masuzaki, O. Motojima, N. Noda and N. Ohyabu,
On the Use of CX Atom Analyzer for Study Characteristics of Ion Component in a LHD Divertor Plasma; Dec. 1996

NIFS-466 H. Miura and S. Kida,
Identification of Tubular Vortices in Complex Flows; Dec. 1996

NIFS-467 Y. Takeiri, Y. Oka, M. Osakabe, K. Tsumori, O. Kaneko, T. Takanashi, E. Asano, T. Kawamoto, R. Akiyama and T. Kuroda,
Suppression of Accelerated Electrons in a High-current Large Negative Ion Source; Dec. 1996

NIFS-468 A. Sagara, Y. Hasegawa, K. Tsuzuki, N. Inoue, H. Suzuki, T. Morisaki, N. Noda, O. Motojima, S. Okamura, K. Matsuoka, R. Akiyama, K. Ida, H. Idei, K. Iwasaki, S. Kubo, T. Minami, S. Morita, K. Narihara, T. Ozaki, K. Sato, C. Takahashi, K. Tanaka, K. Toi and I. Yamada,

Real Time Boronization Experiments in CHS and Scaling for LHD; Dec. 1996

NIFS-469 V.L. Vdovin. T.Watari and A. Fukuyama,
3D Maxwell-Vlasov Boundary Value Problem Solution in Stellarator Geometry in Ion Cyclotron Frequency Range (final report); Dec. 1996

NIFS-470 N. Nakajima, M. Yokoyama, M. Okamoto and J. Nührenberg,
Optimization of M=2 Stellarator; Dec. 1996

NIFS-471 A. Fujisawa, H. Iguchi, S. Lee and Y. Hamada,
Effects of Horizontal Injection Angle Displacements on Energy Measurements with Parallel Plate Energy Analyzer; Dec. 1996

NIFS-472 R. Kanno. N. Nakajima, H. Sugama, M. Okamoto and Y. Ogawa,
Effects of Finite-β and Radial Electric Fields on Neoclassical Transport in the Large Helical Device; Jan. 1997

NIFS-473 S. Murakami, N. Nakajima. U. Gasparino and M. Okamoto,
Simulation Study of Radial Electric Field in CHS and LHD; Jan. 1997

NIFS-474 K. Ohkubo, S. Kubo, H. Idei, M. Sato, T. Shimozuma and Y. Takita,
Coupling of Tilting Gaussian Beam with Hybrid Mode in the Corrugated Waveguide; Jan. 1997

NIFS-475 A. Fujisawa, H. Iguchi, S. Lee and Y. Hamada,
Consideration of Fluctuation in Secondary Beam Intensity of Heavy Ion Beam Prove Measurements: Jan. 1997

NIFS-476 Y. Takeiri, M. Osakabe, Y. Oka, K. Tsumori, O. Kaneko, T. Takanashi, E. Asano, T. Kawamoto, R. Akiyama and T. Kuroda,
Long-pulse Operation of a Cesium-Seeded High-Current Large Negative Ion Source; Jan. 1997

NIFS-477 H. Kuramoto, K. Toi, N. Haraki, K. Sato, J. Xu, A. Ejiri, K. Narihara, T. Seki, S. Ohdachi, K. Adati, R. Akiyama, Y. Hamada, S. Hirokura, K. Kawahata and M. Kojima,
Study of Toroidal Current Penetration during Current Ramp in JIPP T-IIU with Fast Response Zeeman Polarimeter; Jan., 1997

NIFS-478 H. Sugama and W. Horton.
Neoclassical Electron and Ion Transport in Toroidally Rotating Plasmas; Jan. 1997

NIFS-479 V.L. Vdovin and I.V. Kamenskij,
3D Electromagnetic Theory of ICRF Multi Port Multi Loop Antenna; Jan. 1997

NIFS-480 W.X. Wang, M. Okamoto, N. Nakajima, S Murakami and N. Ohyabu,
Cooling Effect of Secondary Electrons in the High Temperature Divertor

Operation, Feb. 1997

NIFS-481 K. Itoh, S.-I. Itoh, H. Soltwisch and H.R. Koslowski,
Generation of Toroidal Current Sheet at Sawtooth Crash; Feb. 1997

NIFS-482 K. Ichiguchi,
Collisionality Dependence of Mercier Stability in LHD Equilibria with Bootstrap Currents; Feb. 1997

NIFS-483 S. Fujiwara and T. Sato,
Molecular Dynamics Simulations of Structural Formation of a Single Polymer Chain: Bond-orientational Order and Conformational Defects; Feb. 1997

NIFS-484 T. Ohkawa,
Reduction of Turbulence by Sheared Toroidal Flow on a Flux Surface; Feb. 1997

NIFS-485 K. Narihara, K. Toi, Y. Hamada, K. Yamauchi, K. Adachi, I. Yamada, K. N. Sato, K. Kawahata, A. Nishizawa, S. Ohdachi, K. Sato, T. Seki, T. Watari, J. Xu, A. Ejiri, S. Hirokura, K. Ida, Y. Kawasumi, M. Kojima, H. Sakakita, T. Ido, K. Kitachi, J. Koog and H. Kuramoto,
Observation of Dusts by Laser Scattering Method in theJIPPT-IIU Tokamak Mar. 1997

NIFS-486 S. Bazdenkov, T. Sato and The Complexity Simulation Group,
Topological Transformations in Isolated Straight Magnetic Flux Tube; Mar. 1997

NIFS-487 M. Okamoto,
Configuration Studies of LHD Plasmas; Mar. 1997

NIFS-488 A. Fujisawa, H. Iguchi, H. Sanuki, K. Itoh, S. Lee, Y. Hamada, S. Kubo, H. Idei, R. Akiyama, K. Tanaka, T. Minami, K. Ida, S. Nishimura, S. Morita, M. Kojima, S. Hidekuma, S.-I. Itoh, C. Takahashi, N. Inoue, H. Suzuki, S. Okamura and K. Matsuoka,
Dynamic Behavior of Potential in the Plasma Core of the CHS Heliotron/Torsatron; Apr. 1997

NIFS-489 T. Ohkawa,
Pfirsch - Schlüter Diffusion with Anisotropic and Nonuniform Superthermal Ion Pressure; Apr. 1997

NIFS-490 S. Ishiguro and The Complexity Simulation Group,
Formation of Wave-front Pattern Accompanied by Current-driven Electrostatic Ion-cyclotron Instabilities; Apr. 1997

NIFS-491 A. Ejiri, K. Shinohara and K. Kawahata,
An Algorithm to Remove Fringe Jumps and its Application to Microwave Reflectometry; Apr. 1997

NIFS-492 K. Ichiguchi, N. Nakajima, M. Okamoto,
Bootstrap Current in the Large Helical Device with Unbalanced Helical Coil Currents; Apr. 1997

NIFS-493 S. Ishiguro. T. Sato, H. Takamaru and The Complexity Simulation Group,
V-shaped dc Potential Structure Caused by Current-driven Electrostatic Ion-cyclotron Instability; May 1997

NIFS-494 K. Nishimura. R. Horiuchi, T. Sato,
Tilt Stabilization by Energetic Ions Crossing Magnetic Separatrix in Field-Reversed Configuration; June 1997

NIFS-495 T. -H. Watanabe and T. Sato,
Magnetohydrodynamic Approach to the Feedback Instability; July 1997

NIFS-496 K. Itoh, T. Ohkawa, S. -I.Itoh, M. Yagi and A. Fukuyama
Suppression of Plasma Turbulence by Asymmetric Superthermal Ions; July 1997

NIFS-497 T. Takahashi, Y. Tomita, H. Momota and Nikita V. Shabrov,
Collisionless Pitch Angle Scattering of Plasma Ions at the Edge Region of an FRC; July 1997

NIFS-498 M. Tanaka, A.Yu Grosberg, V.S. Pande and T. Tanaka,
Molecular Dynamics and Structure Organization in Strongly-Coupled Chain of Charged Particles; July 1997

NIFS-499 S. Goto and S. Kida,
Direct-interaction Approximation and Reynolds-number Reversed Expansion for a Dynamical System; July 1997

NIFS-500 K. Tsuzuki, N. Inoue, A. Sagara, N. Noda, O. Motojima, T. Mochizuki, T. Hino and T. Yamashina,
Dynamic Behavior of Hydrogen Atoms with a Boronized Wall; July 1997

NIFS-501 I. Viniar and S. Sudo,
Multibarrel Repetitive Injector with a Porous Pellet Formation Unit; July 1997

NIFS-502 V. Vdovin, T. Watari and A. Fukuyama,
An Option of ICRF Ion Heating Scenario in Large Helical Device; July 1997

NIFS-503 E. Segre and S. Kida,
Late States of Incompressible 2D Decaying Vorticity Fields; Aug. 1997

NIFS-504 S. Fujiwara and T. Sato,
Molecular Dynamics Simulation of Structural Formation of Short Polymer Chains; Aug. 1997